Progress In Electromagnetics Research M, Vol. 86, 135–144, 2019

Polycarbonate Based Overlapped Architecture for Landscape and Portrait Modes of mmWave 5G Smartphone

Gulur S. Karthikeya*, Mahesh P. Abegaonkar, and Shiban K. Koul

Abstract—In this paper, a low-cost polycarbonate substrate is used for the design of antennas operating in the 28 GHz band. First, a corner bent inset fed patch antenna is proposed with a forward gain of 7 dBi and a front to back ratio of more than 18 dB indicating minimal radiation towards the user post-integration with a mobile terminal. In order to cater to the landscape mode, a corner bent tapered slot antenna is also proposed with a gain of 7 dBi. An overlapped architecture is investigated to demonstrate orthogonal pattern diversity with an effective radiating volume of $0.12\lambda^3$, a port to port distance of 0.13λ at 28 GHz, and mutual coupling of less than 27 dB without deterioration in the pattern integrity of the corresponding modes. Detailed simulated and measured results are presented with justification.

1. INTRODUCTION

In order to cater to the needs of the ever-growing demand for bandwidth hungry wireless applications, researchers across the planet opine that millimeter wave carrier frequencies might ease the spectral congestion in existent commercial cellular systems [1]. The 28 GHz band is projected as one of the candidate bands for future 5G cellular communication networks [2]. The primary issue with deployment of radios at 28 GHz is the relatively higher path loss than its 4G counterpart [3]. The famous testing campaign of researchers at NYU [4] also proves that 28 GHz band might be a feasible choice as long as the maximum distance between the transmitter and receiver is 200 m even in an urban environment. However, the challenge is to mitigate free space path loss by incorporating high gain antennas on transceivers.

Antennas for mobile terminals must have the following features: compatibility with industry standard manufacturing process for high volume production at lower cost per unit, least physical footprint, low radiation towards the user hence leading to low value of specific absorption rate and high gain yield for low effective radiating volume [5]. It must also be observed that the real-estate for antenna integration in a typical commercial smartphones is very limited as demonstrated in [6].

Hence, antenna elements which occupy least volume with high gain would be desired especially at operating frequencies around 28 GHz. The CPW-fed conformal antenna designs proposed in [7, 8] need additional reflector and hence might not be favorable for integration with the standard microstrip-based ecosystem of the RF front-end module. In order to design flexible antennas, several approaches have been reported. For instance, Polyethylene Terephthalate (PET) substrate was used in [9], but the dielectric loss tangent is 0.022 leading to a poor gain yield. For a standard inset fed patch antenna operating at 28 GHz, the boresight gain is 8 dBi when the dielectric loss tangent of the substrate is 0.0009. Similarly, the boresight gain decreases to 5.7 dBi when PET is used as a substrate. Thus, a flexible, low dielectric loss, low-cost substrate is a preferred candidate for antenna designs at Ka band. It must be noted that the liquid crystal polymer (LCP) antenna illustrated in [10] requires an expensive substrate in addition to complicated non-industry standard manufacturing process indicating a poor cost

Received 23 August 2019, Accepted 6 November 2019, Scheduled 19 November 2019
* Corresponding author: Gulur Sadananda Karthikeya (karthikeyaglr@gmail.com).
The authors are with the Centre for Applied Research in Electronics (CARE), IIT Delhi, New Delhi, India.

to volume ratio. Even though the fabrication of the 3D-printed antenna demonstrated in [11] has low cost with low dielectric loss tangent, the selective metallization of the radiator requires time-consuming and expensive inkjet printing with silver thick-film paste. Hence, an antenna design based on a flexible, low-cost polycarbonate substrate is proposed in this paper. The industry standard chemical etching is used for circuit fabrication on the substrate. The typical usage modes of smartphones are portrait and landscape modes as illustrated in Fig. 1. Popular design approaches such as phased arrays would suffer from severe scanning loss when being excited in orthogonal modes [12, 13] leading to unequal gains in both the modes. The shared ground design with pattern diversity would lead to larger physical footprint. Thus, an overlapped design with electrically close ports and orthogonal pattern diversity using corner bent antennas is proposed in this paper.

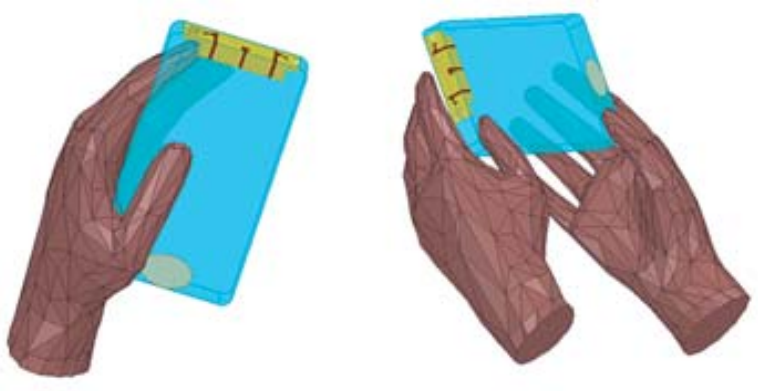

Figure 1. Portrait and Landscape modes of operation.

2. PORTRAIT MODE: CORNER BENT PATCH ANTENNA

The schematic of the proposed corner bent inset fed patch antenna along with a photograph of the fabricated prototype is depicted in Fig. 2. The chosen substrate is 500 µm polycarbonate with ε_r of 2.9 and dielectric loss tangent of 0.01. The chosen substrate is a compromise between cost and flexibility. Also, electrically thinner substrates with low dielectric constant require supporting structures which would in turn compromise the physical footprint and forward gain. The feed-line of the proposed antenna is the standard 50 Ω line feeding the strongly resonant patch antenna. The width of the antenna is chosen to mount the Southwest end-launch connector.

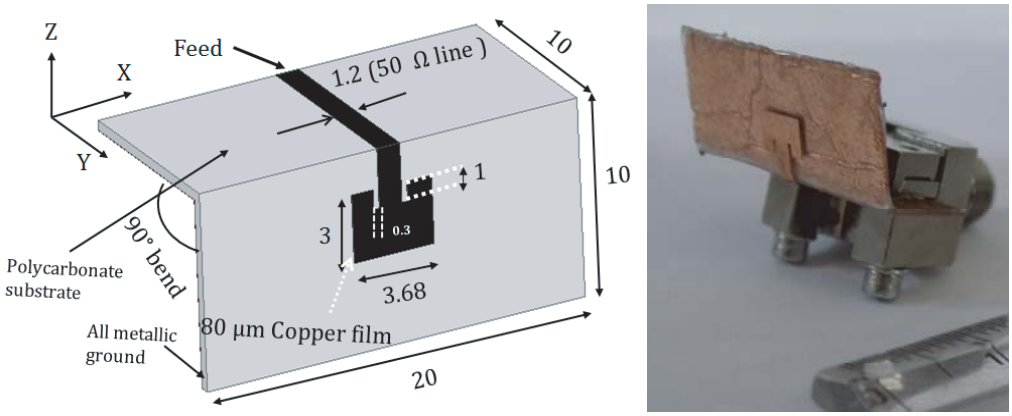

Figure 2. Schematic and photograph of the corner bent patch (Units: mm).

The steps for fabrication are given below:

1. The required dimensions of the polycarbonate is cut.
2. Copper tape of thickness 80 µm is pasted carefully without air bubbles on both sides of the substrate.
3. Industry standard chemical etching process is carried out on the top plane.
4. The edge of the feed-line and the ground planes are filed for better contact with the high frequency connector.

Since the substrate and process are inexpensive, the antenna would yield low cost per unit, when being mass produced. The radiator is at least 1λ away from the feed plane to reduce the effect of the electrically large connector [14]. A corner bend is introduced with the radiator, hence the transmission line lies in the orthogonal plane with respect to the radiator thereby decreasing the physical footprint of the antenna post-integration with the mobile panel. Since the substrate is flexible, minimal discontinuity is created in the overall geometry of the antenna, and copper tape is more flexible than the conventional chemical vapor deposited (CVD) substrate. Since the radiator is bent with the ground plane, there is no requirement of additional FSS based reflectors as reported in [7, 8].

The input reflection coefficient is depicted in Fig. 3. The impedance bandwidth is from 27 to 29 GHz, i.e., 7.2% which is calculated using the equation $2(f_2 - f_1)/(f_2 + f_1)$ where f_1 is 27 GHz, and

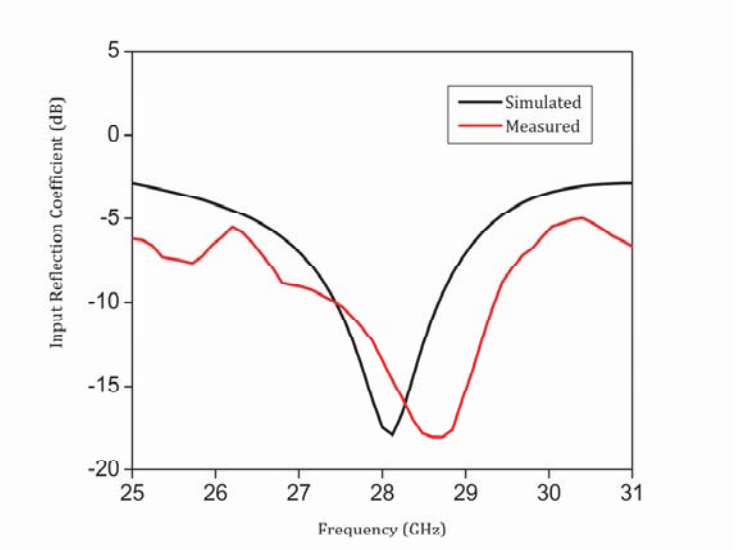

Figure 3. Reflection coefficient of corner bent patch antenna.

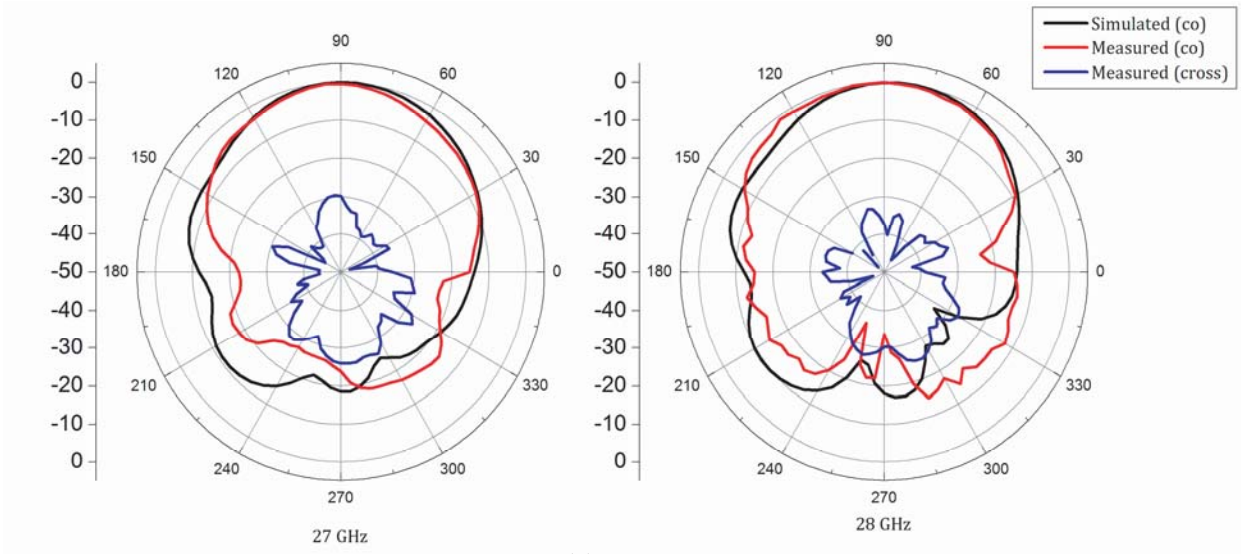

(a)

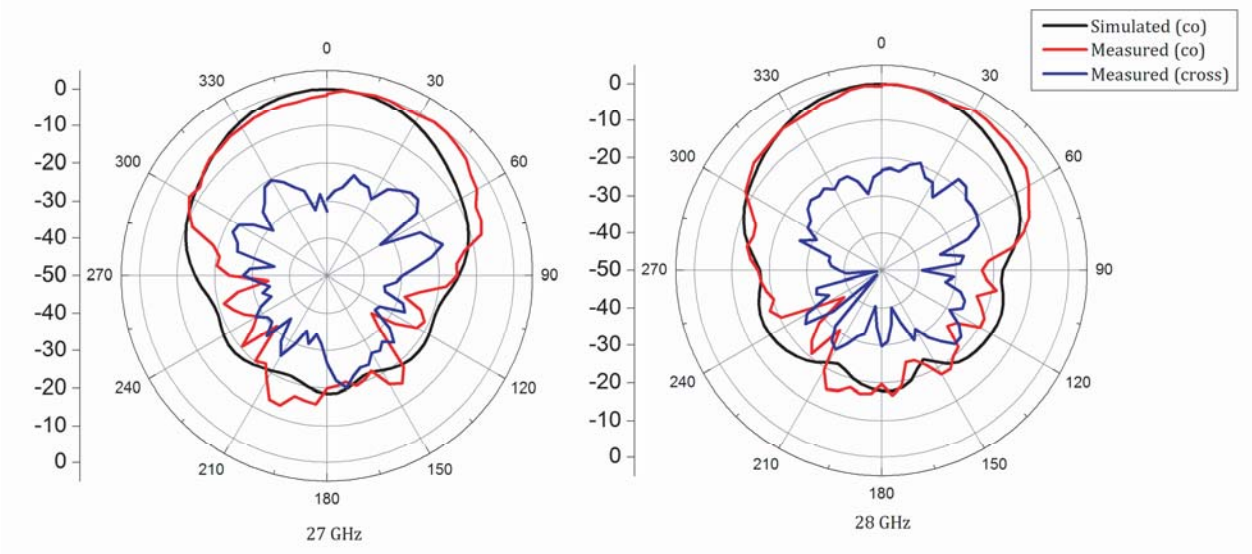

(b)

Figure 4. Radiations patterns at 27 and 28 GHz in (a) YZ, (b) XY planes.

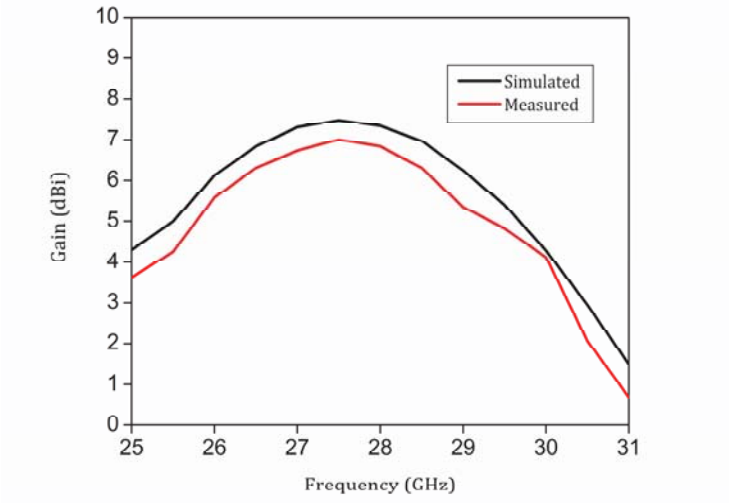

Figure 5. Forward gain of the proposed antenna.

f_2 is 29 GHz, the 10 dB cutoff points from the input reflection coefficient curve. The variation between simulated and measured curves could be attributed to the discontinuity of the trace of the connector and that of the antenna. The dielectric constant of the polycarbonate substrate might have deviated from the values assumed in simulations. The bandwidth could be further increased by increasing the effective radiating volume which leads to a compromise in the physical footprint. Hence, the proposed design is a compact antenna with high forward gain, which is essential for antennas to be integrated with future mobile terminals. The S-parameter measurements are done using Agilent PNA E8364C. All the full-wave simulations are carried out using Ansys HFSS. The simulated and measured radiation patterns in the principal orthogonal plane cuts are shown in Fig. 4. The beamwidth in the YZ plane is 65°, and that in XY plane is 62° at 28 GHz. The front to back ratio is close to 18 dB indicating low value of radiating power towards the user when the antenna is integrated with a mobile terminal.

The forward gain is close to 7 dBi at 28 GHz as observed in Fig. 5. The pattern integrities pre and post bending are almost identical, proving the utility of the flexible polycarbonate substrate.

3. LANDSCAPE MODE: CORNER BENT TAPERED SLOT ANTENNA

The corner bent antenna presented in Section 2 would be operational for portrait mode. In order to cater to the landscape mode, corner bent end fire radiator is investigated in this section. The proposed corner bent tapered slot antenna (TSA) along with its photograph of the fabricated prototype is illustrated in Fig. 6. The feed is a standard 50 Ω line leading to the microstrip to slotline transition through a couple of stepped impedance transformers. The aperture is designed in such a way that the gain is reasonably high with least physical footprint. It must also be noted that since the aperture is optically transparent, solar operated module could also be integrated when the user operates the smartphone in landscape mode.

The simulated and measured input reflection coefficients are shown in Fig. 7. The 10-dB impedance bandwidth is 25 to 29.5 GHz translating to 16.5%. The bandwidth could be further increased by additional balun but at the cost of deterioration in pattern integrity across the band. The discrepancy between simulated and measured curves might be due to manufacturing errors and lack of soldering between the antenna and the end-launch connector.

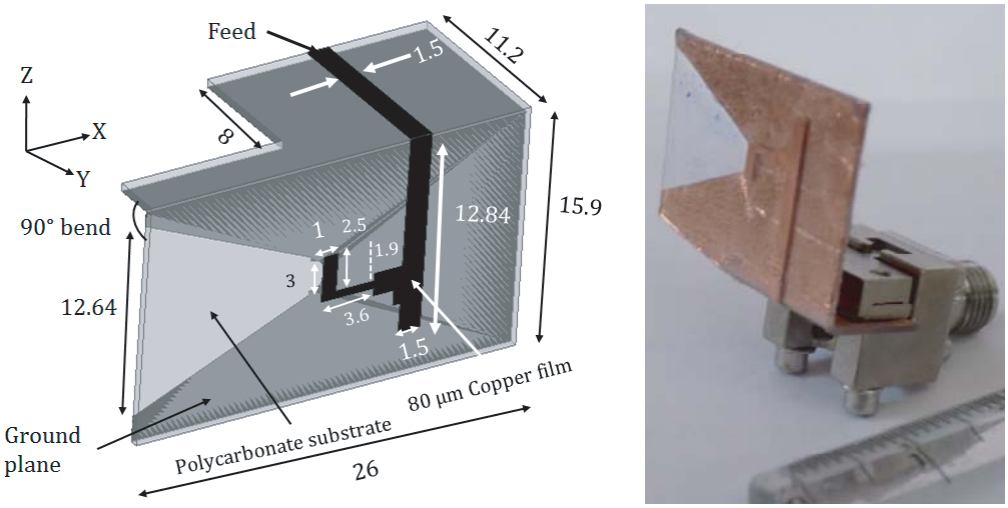

Figure 6. Schematic and photograph of corner bent TSA (Units: mm).

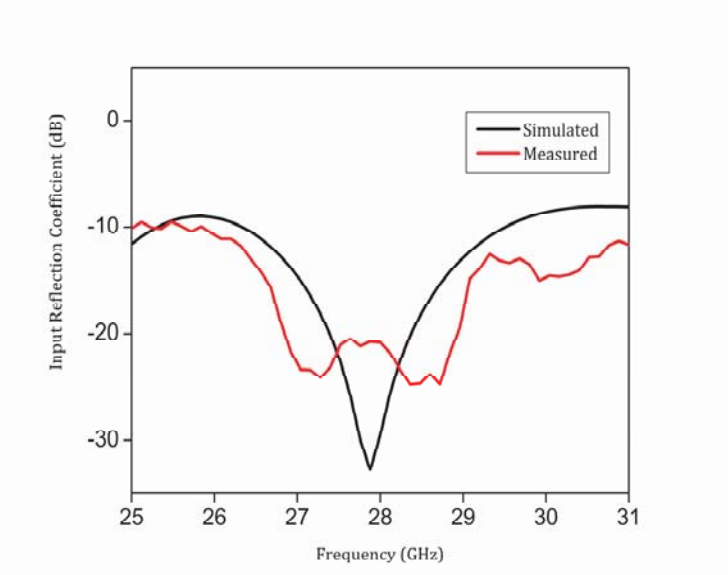

Figure 7. Reflection coefficient of corner bent TSA.

The radiation patterns are shown in Fig. 8 in both principal cuts of the corner bent TSA. The front to back ratio is greater than 10 dB due to the electrically large ground plane thus preventing radiation towards the user when the antenna is integrated onto a mobile terminal. The forward gain is illustrated in Fig. 9, indicating a gain of 7 dBi at 28 GHz. The variation between simulated and measured gains might be due to polarization alignment errors during gain measurement by two-antenna method.

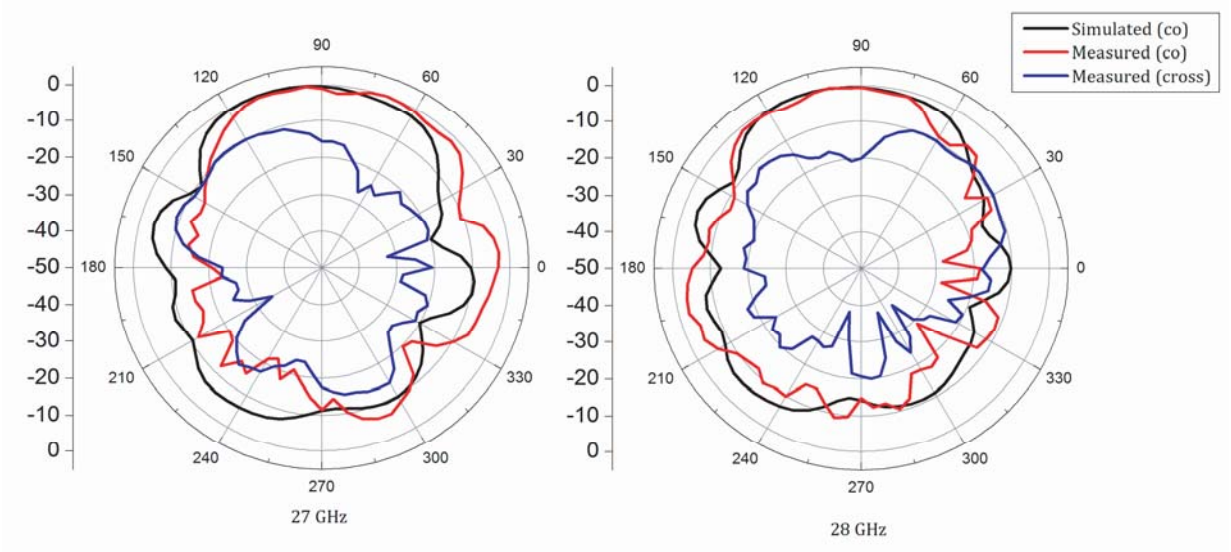

(a)

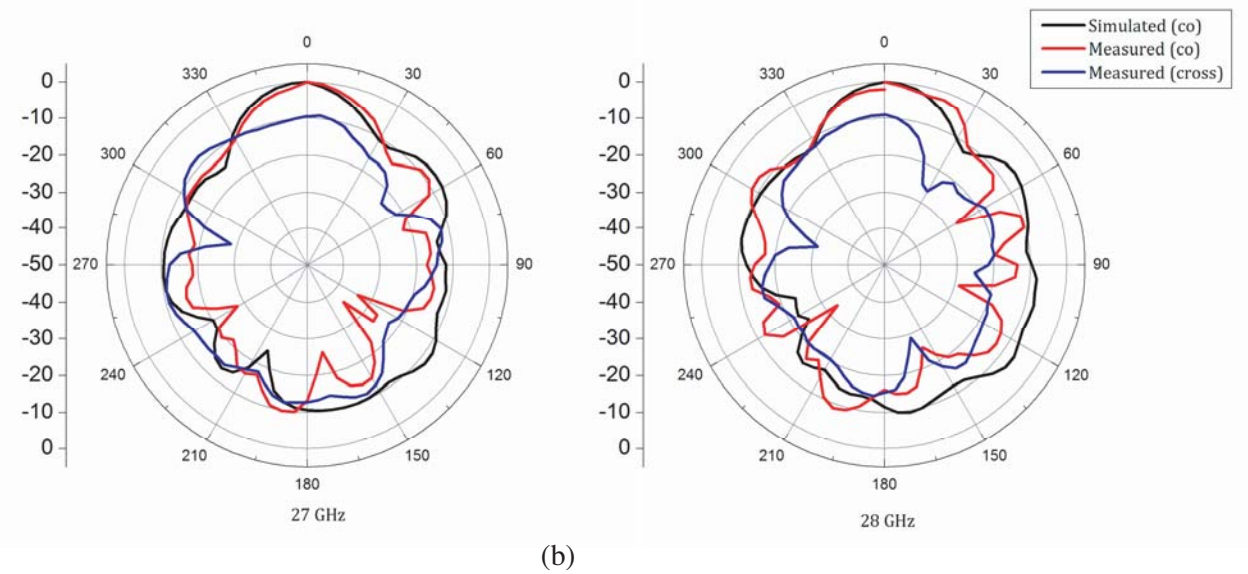

(b)

Figure 8. Radiations patterns at 27 and 28 GHz in (a) XY, (b) XZ planes.

4. OVERLAPPED ORTHOGONAL PATTERN DIVERSITY MODULE

In order to integrate both the proposed antennas, an overlapped architecture is demonstrated as shown in Fig. 10. Both the corner bent antennas are bonded via 3D-printed scaffolding of thickness 1.4 mm, translating to a port-to-port distance of 0.13λ at 28 GHz with minimal distortion in the patterns when the corresponding port is excited. The mutual coupling between the electrically close ports is less than 27 dB as observed in Fig. 11.

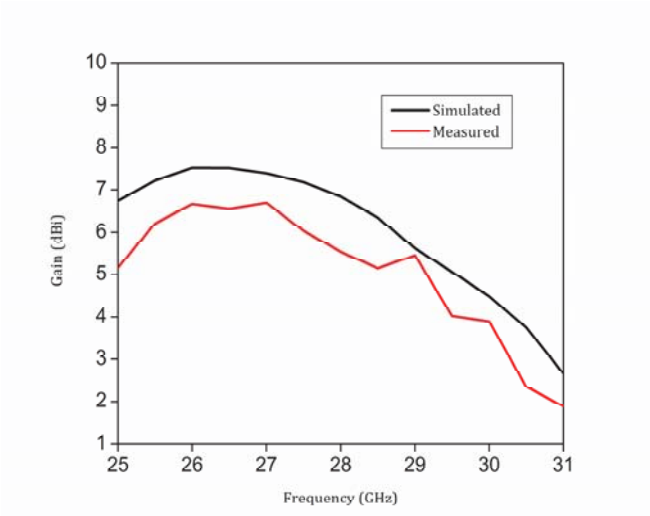

Figure 9. Forward gain of the proposed corner bent TSA.

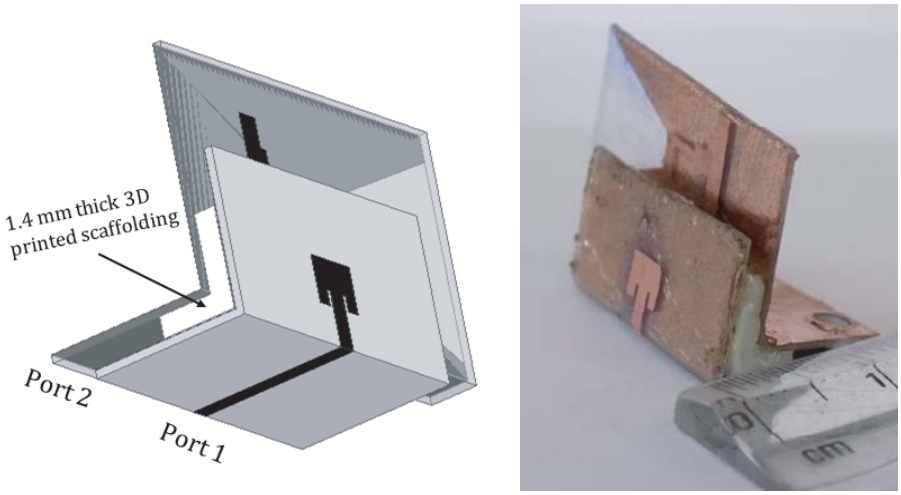

Figure 10. Schematic of the overlapped pattern diversity module.

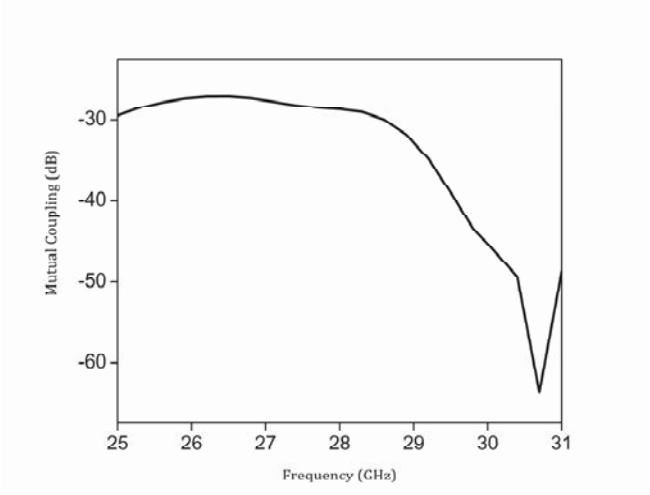

Figure 11. Mutual coupling of the overlapped module.

The patterns retain their integrity in spite of being integrated electrically close as evident from the patterns at 28 GHz in Fig. 12. Port 1 corresponds to the corner bent patch, and port 2 corresponds to the tapered slot antenna. It must also be observed that since the ground plane of the patch antenna is operating as a natural decoupling network, the pattern distortion is minimal. Also, the E-plane patterns of the TSA are almost identical to the stand-alone element. However, the H-plane pattern is slightly deteriorated due to the obstructing radiator. Since the module is electrically compact the compromise in patterns is justified.

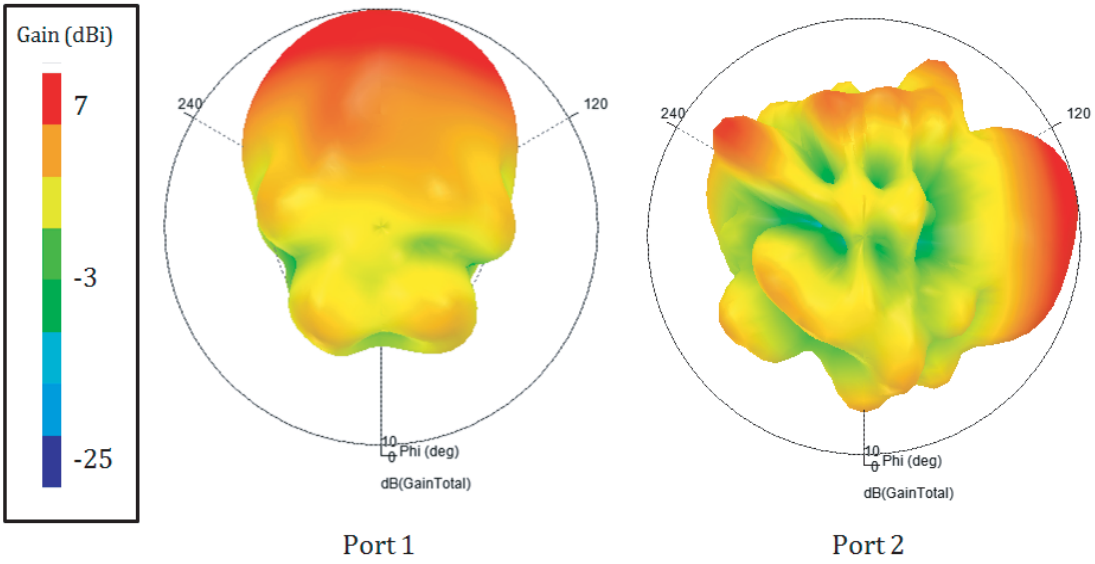

Figure 12. 3D patterns of the overlapped module at 28 GHz.

Table 1 illustrates the utility of the proposed overlapped orthogonal pattern diversity module. It is evident that the module occupies minimum volume with reasonably high gain with orthogonal pattern diversity.

Table 1. Comparison between the proposed module with other reported schemes.

REF	F	G	Con.	MC	ERV	PD
[15]	28	9	No	NA	0.138	$+40°, -40°$
[16]	16	8.5	No	25	0.14	$0°$, $180°$, $\pm 90°$
[17]	10	14	No	NA	0.04	No
[18]	2.5	6.1	No	42	0.116	No
[19]	5.8	4	No	20	0.016	$0°$, $\pm 90°$
[20]	60	12	No	20	1.09	$+35°, -35°$
[21]	60	20	No	30	68.64	$0°$, $+30°$, $-30°$
[22]	64	11	No	NA	0.08	No
[23]	28	11	No	16	0.05	$0°$, $+30°$, $-30°$
Proposed	**28**	**7**	**Yes**	**30**	**0.12**	**0°, 90°**

*F = Centre Frequency (GHz), G = Gain (dBi), Con. = Conformal, MC = Mutual Coupling (dB), ERV = Effective radiating volume (λ^3), PD = Pattern diversity

5. CONCLUSION

Corner bent inset fed patch antenna and tapered slot antenna operating at 28 GHz designed on a low-cost polycarbonate substrate for future 5G mobile terminals is presented. The industry standard low-cost chemical etching process is used for fabrication of the prototypes. An overlapped orthogonal pattern diversity module is also presented which yields a gain of 7 dBi for both portrait and landscape modes of operations with a mutual coupling of less than 28 dB in spite of being electrically close to each other. Hence, the proposed module might be a candidate for mass produced 5G antennas.

REFERENCES

1. Pi, Z. and F. Khan, "An introduction to millimeter-wave mobile broadband systems," *IEEE Communications Magazine*, Vol. 49, No. 6, 101–107, June 2011.
2. Hong, W., K. Baek, Y. Lee, Y. Kim, and S. Ko, "Study and prototyping of practically large-scale mmWave antenna systems for 5G cellular devices," *IEEE Communications Magazine*, Vol. 52, No. 9, 63–69, September 2014.
3. Friis, H. T., "A note on a simple transmission formula," *Proceedings of the IRE*, Vol. 34, No. 5, 254–256, May 1946.
4. Rappaport, T. S., et al., "Millimeter wave mobile communications for 5G cellular: It will work!," *IEEE Access*, Vol. 1, 335–349, 2013.
5. Rowell, C. and E. Y. Lam, "Mobile-phone antenna design," *IEEE Antennas and Propagation Magazine*, Vol. 54, No. 4, 14–34, Aug. 2012.
6. Huo, Y., X. Dong, and W. Xu, "5G cellular user equipment: From theory to practical hardware design," *IEEE Access*, Vol. 5, 13992–14010, 2017.
7. Karthikeya, G. S., M. P. Abegaonkar, and S. K. Koul, "CPW fed wideband corner bent antenna for 5G mobile terminals," *IEEE Access*, Vol. 7, 10967–10975, 2019.
8. Karthikeya, G. S., M. P. Abegaonkar, and S. K. Koul, "CPW fed conformal folded dipole with pattern diversity for 5G mobile terminals," *Progress In Electromagnetics Research C*, Vol. 87, 199–212, 2018.
9. Jilani, S. F. and A. Alomainy, "Planar millimeter-wave antenna on low-cost flexible PET substrate for 5G applications," *2016 10th European Conference on Antennas and Propagation (EuCAP)*, 1–3, Davos, 2016.
10. Jilani, S. F., M. O. Munoz, Q. H. Abbasi, and A. Alomainy, "Millimeter-wave liquid crystal polymer based conformal antenna array for 5G applications," *IEEE Antennas and Wireless Propagation Letters*, Vol. 18, No. 1, 84–88, Jan. 2019.
11. Hawatmeh, D. F., S. LeBlanc, P. I. Deffenbaugh, and T. Weller, "Embedded 6-GHz 3-D printed half-wave dipole antenna," *IEEE Antennas and Wireless Propagation Letters*, Vol. 16, 145–148, 2017.
12. Ta, S. X., H. Choo, and I. Park, "Broadband printed-dipole antenna and its arrays for 5G applications," *IEEE Antennas and Wireless Propagation Letters*, Vol. 16, 2183–2186, 2017.
13. Zhu, S., H. Liu, Z. Chen, and P. Wen, "A compact gain-enhanced Vivaldi antenna array with suppressed mutual coupling for 5G mmWave application," *IEEE Antennas and Wireless Propagation Letters*, Vol. 17, No. 5, 776–779, May 2018.
14. Alhalabi, R. A. and G. M. Rebeiz, "High-efficiency angled-dipole antennas for millimeter-wave phased array applications," *IEEE Transactions on Antennas and Propagation*, Vol. 56, No. 10, 3136–3142, 2008.
15. Yang, B., Z. Yu, Y. Dong, J. Zhou, and W. Hong, "Compact tapered slot antenna array for 5G millimeter-wave massive MIMO systems," *IEEE Transactions on Antennas and Propagation*, Vol. 65, No. 12, 6721–6727, December 2017.
16. Reddy, G. S., A. Kamma, S. Kharche, J. Mukherjee, and S. K. Mishra, "Cross-configured directional UWB antennas for multidirectional pattern diversity characteristics," *IEEE Transactions on Antennas and Propagation*, Vol. 63, No. 2, 853–858, February 2015.

17. Zhou, B., H. Li, X. Zou, and T.-J. Cui, "Broadband and high-gain planar Vivaldi antennas based on inhomogeneous anisotropic zero-index metamaterials," *Progress In Electromagnetics Research*, Vol. 120, 235–247, 2011.
18. Liu, F., J. Guo, L. Zhao, X. Shen, and Y. Yin, "A meta-surface decoupling method for two linear polarized antenna array in sub-6 GHz base station applications," *IEEE Access*, Vol. 7, 2759–2768, 2019.
19. Sharma, Y., D. Sarkar, K. Saurav, and K. V. Srivastava, "Three-element MIMO antenna system with pattern and polarization diversity for WLAN applications," *IEEE Antennas and Wireless Propagation Letters*, Vol. 16, 1163–1166, 2017.
20. Dadgarpour, A., B. Zarghooni, B. S. Virdee, and T. A. Denidni, "One- and two-dimensional beam-switching antenna for millimeter-wave MIMO applications," *IEEE Transactions on Antennas and Propagation*, Vol. 64, No. 2, 564–573, February 2016.
21. Briqech, Z., A. Sebak, and T. A. Denidni, "Wide-scan MSC-AFTSA array-fed grooved spherical lens antenna for millimeter-wave MIMO applications," *IEEE Transactions on Antennas and Propagation*, Vol. 64, No. 7, 2971–2980, July 2016.
22. Sun, M., Z. N. Chen, and X. Qing, "Gain enhancement of 60-GHz antipodal tapered slot antenna using zero-index metamaterial," *IEEE Transactions on Antennas and Propagation*, Vol. 61, No. 4, 1741–1746, April 2013.
23. Wani, Z., M. P. Abegaonkar, and S. K. Koul, "Millimeter-wave antenna with wide-scan angle radiation characteristics for MIMO applications," *Int. J. RF Microw. Comput. Aided Eng.*, e21564, 2018.